Proceedings of the 21st ICSMGE, Vienna, Austria, 14 – 19 June 2026. Pistrol, Adam & Schweiger (eds.)
Published by: ÖGG, Austrian Society for Geomechanics, Salzburg, Austria, ISBN 978-3-9503898-4-5
https://doi.org/10.53243/ICSMGE2026-1142

Advanced finite element modelling for constructible and sustainable surcharge design using prefabricated vertical drains in Port of Brisbane land reclamation

Nay Win, Jarreau Alinur, Darshi Kasturiaratchi
WSP Australia Pty Ltd, Australia, nay.win@wsp.com

Clinton Chan, Zen Ng
Port of Brisbane Pty Ltd, Australia

ABSTRACT: This paper presents an advanced finite element modelling (FEM) study of land reclamation works at the Port of Brisbane, where soft Holocene clays and hydraulically placed dredged mud fill pose significant settlement challenges. A critical zone beneath a containment bund, where prefabricated vertical drains were omitted due to constructability constraints, posed complex consolidation scenario. Due to the limitations associated with conventional 1D consolidation analysis, a more sophisticated 2D FEM model using the Soft Soil Creep (SSC) model was developed and calibrated with analytical benchmarks. The model simulated the full reclamation history and complex drainage interactions, capturing key time-dependent soft soil behaviour, including primary consolidation, strength gain, and creep effects. Validation against field measurements such as CPTu and pore pressure dissipation tests demonstrated good agreement. Findings indicate that settlement performance at the 'missing' PVD zone remains within design limits without requiring further ground treatment. The study demonstrates how 2D FEM numerical models provide more realistic settlement predictions, enabling cost-effective and constructible design decisions in complex reclamation environments.

KEYWORDS: land reclamation, soft soils, prefabricated vertical drains, FEM calibration and validation, sustainable design.

1 INTRODUCTION

The Port of Brisbane (PoB), at the lower reach of the Brisbane River and extending into Moreton Bay, is Queensland's largest general cargo port and a critical freight hub for Southeast Queensland, Australia. To accommodate projected trade growth and population demand, extensive land reclamation works have been undertaken for future expansion.

Reclamation areas are underlain by thick Holocene marine clays of low undrained shear strength, high compressibility, and low permeability, overlain by very soft hydraulically placed dredged mud (DM). Conventional ground improvement, prefabricated vertical drains (PVDs) and surcharging, is routinely applied to accelerate consolidation, improve strength, and control PCS. However, constructability challenges can necessitate deviations from standard practice. In this case study, difficulties installing PVDs through a containment bund between reclamation paddocks created a 'missing' PVD zone, introducing complex drainage interactions, including radial flow toward adjacent PVD zones, perched water tables, and variable fill histories. This paper examines the geotechnical implications of the missing PVD zone, highlighting the limitations of conventional 1D consolidation analysis. The study applies the SSC constitutive model, implements PVD effects in the FEM framework, and validates results against analytical benchmarks and field data.

Figure 1. Overview of the Port of Brisbane and its regional context

2 GEOLOGICAL AND GEOTECHNICAL SETTING

A summary of the key geological units at PoB that are relevant to this study is provided in Table 1 (Alinur et al., 2023):

Table 1. Geological Units encountered at PoB.

Geological Unit	*Description*
Upper Holocene Clay (UHC)	Predominantly very loose or loose sand with some inter-layered soft clays.
Lower Holocene Clay (LHC)	Normally to slightly over-consolidated, highly compressible, marine clay, during marine transgression at the end of the last glacial period.
Pleistocene	Older over-consolidated sediments, stiff to hard clays and medium dense to dense sands. This layer is considered to be incompressible relative to the overlying Holocene deposits.

Back-analyses and historical settlement monitoring indicate that LHC layer is the primary contributor to both construction and post-construction settlement at the site (Ng et al., 2016). The LHC layer typically extends to depths of up to 30 m. Figure 2 presents the interpreted base of LHC, highlighting the presence of a paleochannel running north–south beneath the Port reclamation area. All reduced levels in this paper refer to metres from Port Datum (PD).

Above the Holocene clay deposits, reclamation paddocks were formed by constructing containment bunds, followed by hydraulic placement of dredged mud fill therein, varying between 6 to 10 m thickness. The dredged materials are under-consolidated, i.e., still undergoing self-weight consolidation after placement and prior to the application of any external loads such as surcharge. They are extremely compressible and exhibit very low undrained shear strength. A sand fill layer is placed to cap the dredged mud, facilitating construction access and PVD installation.

Based on the available geotechnical investigation data, CPTu, obtained during various site investigation campaigns (from 2006 to 2023), Figure 3 presents the typical ground profile for the area of interest (as shown in Figure 2).

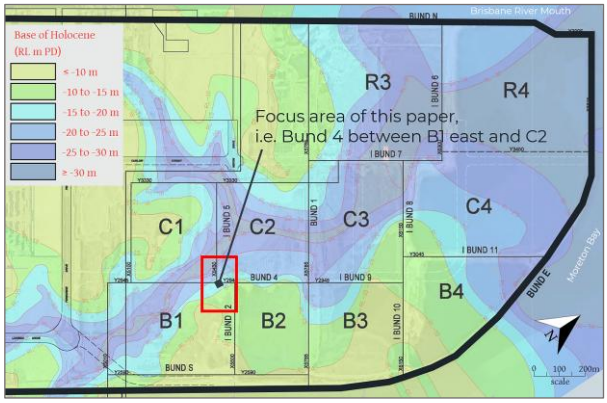

Figure 2. Base of Lower Holocene (soft clay) contours

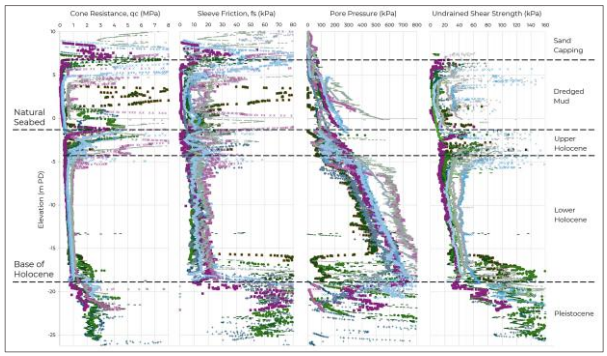

Figure 3. Typical ground profile around B1-East and C2 paddocks

3 OVERVIEW OF LAND RECLAMATION HISTORY AND GROUND IMPROVEMENT DESIGN

3.1 *Project context and reclamation sequence*

The focus of this study is Bund 4, a bund separating the B1 East and C2 reclamation paddocks at PoB. Figure 4 presents a brief aerial overview of land reclamation in the study area. As shown in Figure 5, Bund 4 was constructed in two stages to RL 10, while dredged mud was placed to RL 6.5 in B1 East and to 9.5 in C2. The final site level is RL 8.0, with an allowable PCS limit of 250 mm to support 36 kPa industrial and pavement loading.

Figure 4. Aerial overview of land reclamation at PoB

At the time of the 2023 ground improvement design phase, consolidation in both LHC and dredged mud fill was still ongoing, as excess pore pressures from Bund 4 construction and dredged mud placement had not fully dissipated. Assuming OCR = 1 without accounting for these pressures could underestimate future settlement. Settlement analyses were undertaken in Settle3 using 1D nonlinear consolidation theory, incorporating overconsolidated creep behaviour using the Mesri formulation (Mesri and Castro, 1987). The ground improvement design for B1 East and Bund 4 comprised PVDs at 1.25 m spacing, extending through the LHC into the Pleistocene, combined with surcharging to RL 16 for 18 months. C2 adopted a 1.7 m PVD spacing with a similar surcharge to RL 16. Figure 5 summarises the reclamation history from 2006–2023 alongside the proposed ground improvement works.

3.2 *Constructability constraints*

While PVD installation was completed in most of the B1 East and C2 paddocks, constructability constraints arose within Bund 4. The bund was constructed of compacted sand-clay mix, making conventional PVD installation, by pushing drains through the full thickness, impractical. The design originally proposed pre-drilling the upper 5 to 6 m of the bund before continuing PVD installation through the underlying soft clays; pre-drilling through internal bunds had been the status-quo for previous surcharge campaigns at PoB. However, due to construction challenges, the pre-drilling was not executed as intended, which gave rise to challenging the premise that PVDs were required in a 10 m wide by approximately 200 m long zone beneath Bund 4 (where no PVDs were installed).

3.3 *Impact assessment for missing PVD zone*

A detailed impact assessment was required for the zone beneath Bund 4 where PVD installation was not completed. The objective was to explore if alternative design strategies, such as increasing the surcharge height, or optimising drain spacing, were required, while realistically accounting for the complex drainage interactions in this transition zone. The zone of 'missing' PVDs beneath Bund 4 introduced a complex consolidation scenario. Radial flow toward adjacent drained zones (B1-East and C2), fluctuating perched water tables from surcharging, and differing fill placement histories across adjacent paddocks reduces the applicability of conventional 1D consolidation analyses for accurately capturing ground response in this zone.

To confirm design compliance, a more robust 2D FEM approach was adopted. The FEM model was developed from initial seabed level, incorporating the full reclamation history, as presented in Figure 5, to simulate historical loading, stress changes, and pore pressure generation in the dredge mud and LHC layers. To capture the behaviour of dredge mud by activating soil clusters at appropriate times, i.e., placement of dredge mud fill, the model reproduced excess pore pressure built up under self-weight loading. The parameters adopted for the consolidation analysis, Table 2**,** were derived from laboratory tests and back-analyses of settlement trends from comparable PoB projects (Ng et al., 2016).

Table 2. Summary of design parameters for compressible materials

Parameter	UHC	LHC	DM	*Units*
Bulk unit weight, γ_b	17	16	14.5	kN/m^3
Compression ratio, *CR*	0.10	0.27	0.30	-
CR / *RR*	7.5	7.5	7.5	-
Coefficient of secondary compression, $C_{\alpha e}$	0.4	1.1	1.2	%
Coefficient of vertical consolidation, C_v	5	2	2	m^2/year
Pre-Overburden pressure, *POP*	20-40	20	-	kPa
Cohesion, c'	4	2	1-2	kPa
Friction angle, ϕ	26	22	22	(º)

The POP values presented in Table 2 are representative of the natural Holocene units prior to the initial reclamation works in 2006, including bund and paddock construction.

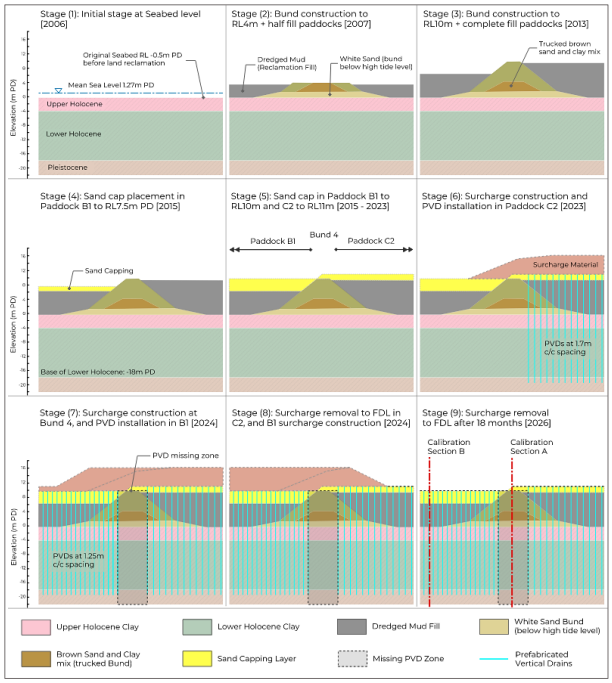

Figure 5. Detail land reclamation sequences from seabed level

4 CALIBRATION AND VALIDATION OF SOFT SOIL BEHAVIOUR IN ADVANCED FEM MODELLING

Prior to developing the 2D model to assess performance of the missing PVD zone, a series of calibration exercises were undertaken to align the FEM parameters with analytical benchmarks and field observations. These included comparisons with analytical solutions for consolidation, modelling of PVD effects, and evaluation of soft soil strength gain trends observed in site investigation data over time. The adopted calibration framework is summarised in Figure 6, with the locations of calibration sections indicated in Figure 5: Section A for consolidation parameter of UHC and LHC layers; and Section B for dredged mud and PVD modelling approach.

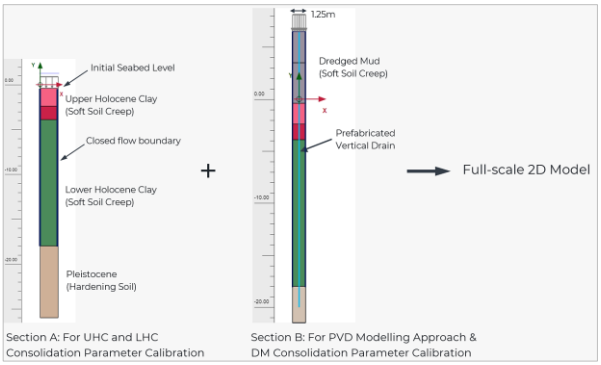

Figure 6. Adopted calibration framework and sections overview

4.1 *Calibration of soft soil behavior in FEM modelling*

While conventional 1D analytical methods based on Terzaghi (linear) and Gibson (non-linear) remain widely used and provide a useful framework, they have limitations in capturing complex, time-dependent soil behaviour and multidimensional flow. To address these, advanced numerical methods incorporating more rigorous constitutive models are often required. The SSC constitutive model in PLAXIS was adopted to simulate the time-dependent behaviour of both the dredged mud and underlying marine clay.

4.1.1 *Primary consolidation in SSC model*

In the SSC framework, compressibility is defined using the modified compression index (λ^*) and swelling index (κ^*), which can be derived from conventional consolidation parameters: the compression index (C_c), recompression index (C_r), and initial void ratio (e_0). The transformation from conventional parameters to the SSC model input values follow established procedures documented in the PLAXIS Material Models Manual (Brinkgreve et al., 2023). As these derivations are widely used and relatively straightforward, they are not elaborated further in this paper.

4.1.2 *Derivation of permeability parameters*

In conventional 1D consolidation theory, C_v governs the rate of pore pressure dissipation and is derived from laboratory or in-situ tests. For coupled flow-deformation analysis using the SSC model, vertical permeability (k_v) must be explicitly provided as a model input. It can be derived from C_v based on a chain of well-established classical soil mechanics relationships:

$$k_v = \frac{C_v \cdot \gamma_w \cdot C_c}{2.3\,(1 + e_0)\,\sigma'_v} \qquad (1)$$

Equation (1) links test-derived parameters C_v, C_c, and e_0 to the permeability input for the SSC model. It also highlights the stress-dependent nature of permeability in soft soils, as the effective vertical stress (σ'_v) directly influences the resulting value of vertical permeability. Using this expression, representative permeability values for the UHC layer and LHC layer that aligned with design C_v values presented in Table 2 were calculated. A horizontal-to-vertical permeability ratio of $k_h / k_v = 2$ was adopted (Ng et al., 2016).

The derived permeability values were validated against analytical solutions through the development of a finite element unit cell model for Section A, as shown in Figure 6. This model was constructed specifically to confirm that permeability values adopted in the FEM are consistent with those adopted in conventional analytical design approach. This calibration step focused solely on the natural permeability of the UHC and LHC layers prior to incorporating the effects of PVDs, which are addressed in Section 4.2. The construction sequence implemented for this calibration corresponds to Stage (1) to (5) of Figure 5. As shown in Figure 7, good agreement was observed between the FEM and analytical approach in terms of the rate of excess pore pressure dissipation (slope of settlement-time) response.

4.1.3 *Creep behaviour and time-dependent modelling*

The onset of secondary compression (creep) in soft soils has long been a subject of discussion in geotechnical literature, typically framed around two commonly referenced hypotheses:

- Hypothesis–A: Creep begins only after primary consolidation is substantially complete.
- Hypothesis–B: Creep occurs concurrently with primary consolidation, starting from the moment of loading.

Current Southeast Queensland practice typically adopts Hypothesis–A for its simplicity and alignment with workflows separating primary and secondary settlement phases. Construction-stage settlement monitoring is common, while post-construction monitoring, needed to isolate creep, is rare. Observed settlements during construction are therefore interpreted as primary consolidation and back-analysed to obtain the compression ratio (CR). If actual behaviour follows Hypothesis–B, this can overestimate CR, and since $C_{\alpha e}$ is often derived empirically from CR (Mesri, 1994), this can in turn result in conservatively high values of $C_{\alpha e}$. The SSC model does not assume a discrete transition between primary and secondary

compression. Instead, it simulates time-dependent deformation using a viscoplastic formulation where creep initiates immediately upon loading and evolves as a function of effective stress, preconsolidation pressure, and elapsed time (Vermeer and Neher, 1999). In conventional soil mechanics and in the Soft Soil constitutive model, OCR is defined as the ratio of preconsolidation pressure (P_p) to the current effective stress (P^{eq}), i.e., OCR = P_p / P^{eq} and remains constant over time for a constant load. The SSC model incorporates an isotropic preconsolidation pressure $P_{p(iso)}$ that evolves with time T_{age} to capture creep deformation. While the primary consolidation is still governed by the traditional yield surface associated with the initial P_p (as derived from input OCR), the time-dependent increase in $P_{p(iso)}$ governs the creep behaviour. To capture this mechanism, the following expression can be derived, where T_{age} is the elapsed time in days, typically measured from the time of deposition, and (μ^*) is the modified creep index:

$$P_{p(iso)} = P^{eq} \cdot (T_{age})^{\frac{\mu^*}{\lambda^* - \kappa^*}} \quad (2)$$

Volumetric strain due to creep ($\Delta\varepsilon_v^c$) over a time increment T_{creep} can be expressed as a function of current stress level:

$$\Delta\varepsilon_v^c = \mu^* . \ln\left[1 + \frac{T_{creep}}{1\ day} \cdot \left(\frac{P^{eq}}{P_{p(iso)}}\right)^{\frac{\lambda^* - \kappa^*}{\mu^*}}\right] \quad (3)$$

Together, these equations illustrate the so-called *ageing effect*, that is, as time progresses, $P_{p(iso)}$ increases as expressed in Equation (2), thereby reducing the P^{eq} / $P_{p(iso)}$ ratio in Equation (3). This reduction decreases volume change due to creep ($\Delta\varepsilon_v^c$), providing a physically meaningful mechanism to simulate the decaying nature of creep over time. This concept is critical for avoiding overestimation of long-term settlement in numerical models when design parameters are based on conventional interpretations using Hypothesis–A. From a practical standpoint, if Hypothesis–A-based parameters (typically with higher CR and $C_{\alpha e}$ values) are directly input into the SSC model, which inherently assumes simultaneous primary and creep strains, the result may be an overprediction of settlement. Rather than recalibrating $C_{\alpha e}$ to fit the SSC formulation which may disrupt established empirical CR– $C_{\alpha e}$ correlations (Mesri, 1994), the ageing concept described above offers an effective alternative.

To implement this, a *dummy* consolidation stage can be introduced at the start of the model, with a defined ageing duration T_{age}. This artificially increases $P_{p(iso)}$ before applying embankment or surcharge loads. During subsequent loading stages, the effective stress P^{eq} increases due to dissipation of excess pore pressure, but the high initial $P_{p(iso)}$ ensures that early creep is minimal. Creep deformation only becomes significant once P_{eq} approaches $P_{p(iso)}$, effectively mimicking Hypothesis–A behaviour, where creep starts only after a certain degree of primary consolidation occurred, within the SSC framework. The duration of this *dummy* ageing stage must be carefully calibrated. Analytical solutions based on Hypothesis–A can be used as benchmarks, while typical geological deposition timelines from regional studies can guide the selection of a representative ageing duration for modelling purposes. Parameters in Table 2 were interpreted within the Hypothesis–A framework. To apply them in SSC, the ageing concept was implemented, by introducing creep into Section A unit-cell model shown in Figure 6, using Stage (1) to (5) from Figure 5, followed by additional years to clearly capture the onset and progression of creep. As shown in Figure 7, applying Hypothesis–A parameters without ageing overestimated, whereas introducing an ageing period representative of the depositional history achieves close agreement with analytical benchmarks. Geological studies of Moreton Bay (Tibbets et al., 1998), LHC was deposited during the marine transgression, with paleo-river channels infilled about 6000–8000 years before present (BP). UHC was deposited later, 1000-3000 years BP, after sea-level stabilisation. This depositional timeline was incorporated as the initial ageing stages, providing a geologically plausible foundation for the SSC formulation.

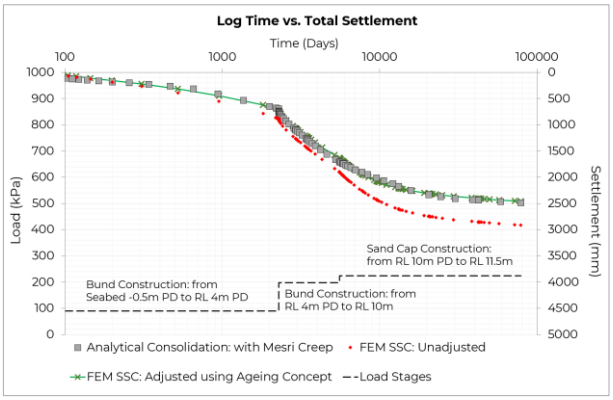

Figure 7. FEM creep calibration with analytical benchmark

4.2 *Calibration of PVD effects in FEM modelling*

The implementation of PVDs in numerical models has been extensively investigated in literature. PVD design parameters for the B1-East area of this project are summarised in Table 3.

Table 3. Design parameters adopted for PVD at B1-East area

Parameter	Symbol	Value	Unit
Pattern	-	Triangular	-
Spacing	S	1250	mm
Width	b	100	mm
Thickness	t	3	mm
Smear zone ratio	$s = d_s / d_w$	5	-
Spacing ratio	$n = D_e / d_w$	25.5	-
Permeability ratio: undisturbed to smear	k_h / k_s	7	-

Commonly adopted methods for simulating PVDs in 2D plane strain FEM include:

1. Equivalent Vertical Permeability: Vertical permeability of the soil layer is increased to cater for wick drains and smear (CUR 191, 1997).
2. Drain Element Approach: zero excess pore pressure elements simulate drain paths, with permeability modified to represent drainage boundary conditions and smear effects. (Indraratna et al., 2005).

Given the availability of excess pore pressure monitoring and the need for close agreement between modelled and observed performance, the second approach was adopted. Equivalent horizontal permeability for plane strain, incorporating PVD geometry and smear, was derived using Indraratna et al. (2005):

$$k_{hp,eq} = k_h \left[\frac{\frac{2}{3}\left(1 - \frac{1}{n}\right)^2}{\ln\left(\frac{n}{s}\right) + \left(\frac{k_h}{k_s}\right)\ln(s) - 0.75}\right] \quad (4)$$

Horizontal permeability values k_h for UHC and LHC layers were derived and validated in Section 4.1.2, while dredge mud permeability was estimated using the same methodology. All were converted to equivalent horizontal permeability using Equation (4), based on PVD parameters from Table 3.

To benchmark the accuracy of drain element approach, results were compared with Barron's (1948) classical radial

consolidation solution. Analytical degrees of consolidation were converted to settlement–time curves and compared with FEM results using equivalent permeability and embedded line drain elements. As shown in Figure 8, the strong agreement confirms that the permeability values for UHC, LHC, and dredge mud from Equation (1), adjusted via Equation (4) for PVD effects, are appropriate.

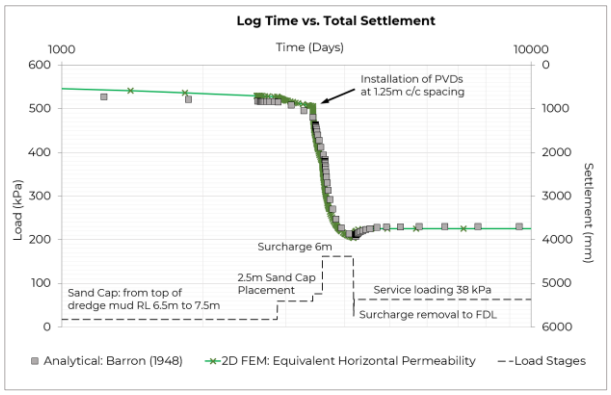

Figure 8. Calibration of PVD modelling with analytical benchmark

4.3 *Validation of soft soil strength gain behavior in FEM*

Following the calibration of compressibility, permeability, and creep parameters in Sections 4.1 and 4.2, this section validates if the FEM model captures strength gain behaviour in the soft soils during consolidation. In highly compressible and normally- or under-consolidated soils with low permeability, such as the dredge mud and LHC layers, the application of external loads, through bund construction, paddock infill, and surcharging, generates excess pore pressures. The dissipation of these pressures over time increases the degree of consolidation, which elevates effective stress and leads to measurable gains in undrained shear strength (S_u). To validate this behaviour, CPTu data from 2006, 2014, 2017, and 2023 were used to interpret S_u in the dredged mud and LHC layers. A unit-cell model (Section B) representing the B1-East paddock was developed with the full staged construction history in Figure 5. S_u values were extracted at the same time points as the CPTu campaigns. Figure 9 shows good agreement between model predictions and field-interpreted values in both dredged mud and LHC layers. This confirms that the predicted time-dependent response from FEM model aligns well with observed site behaviour.

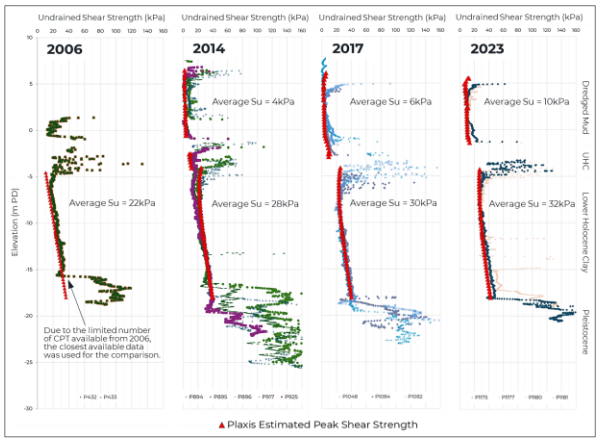

Figure 9. Validation of strength gain behaviour from FEM with CPTu

A key factor in modelling consolidation-induced strength gain is the hydraulic behaviour of the Pleistocene layer beneath the Holocene clays. Comprising interbedded very stiff clays and medium dense sands, it raises the question of whether to model it as a drainage boundary or low permeability confining layer. While sand lenses are present, its overall permeability is likely higher than LHC but closer to UHC. Treating it as fully drained may not accurately reflect its composite behaviour, particularly at the scale relevant to consolidation modelling. Two modelling scenarios were tested: (1) the Pleistocene layer was assigned high permeability, simulating free drainage at the base of the LHC; and (2) it was treated as a clay layer with C_v equivalent to that of the UHC. Shear strength profiles were extracted from both cases for 2017 and compared to CPTu data as presented in Figure 10. The results indicate that assuming free drainage at the base leads to accelerated consolidation in the LHC and overestimation of strength gain. The low-permeability case aligned more closely with the interpreted field behaviour, indicating that consolidation was more restricted from below. This supports the treatment of the Pleistocene as a low-permeability boundary in this context.

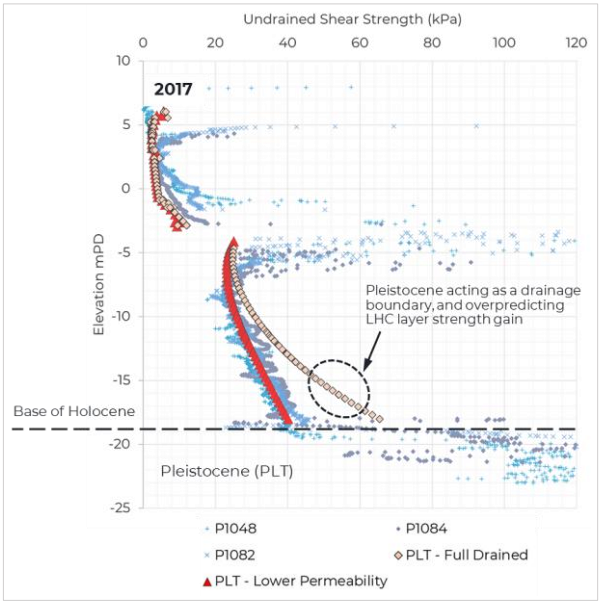

Figure 10. Indication of Pleistocene permeability impact on LHC

5 IMPACT ASSESSMENT & DESIGN OPTIMISATION

Prior to developing the full-scale 2D FEM model, Section 4 established the soft soil behaviour and PVD modelling approach using unit-cell model calibration with analytical benchmarks. Validation against field measurements also confirmed the reliability of the selected SSC parameters. This section presents the development of the full 2D model.

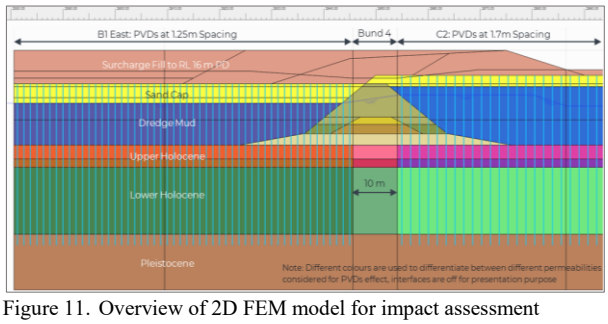

Figure 11. Overview of 2D FEM model for impact assessment

The SSC model was adopted for the dredged mud, UHC and LHC layers, with parameters summarised Table 2, derived as described in Section 4. It simulates the staged reclamation history, Figure 5, with PVDs activated at relevant stages, and equivalent permeability assigned to capture drain effects. The Site investigation in 2023, CPTu and dissipation tests in

paddock B1-East, provided data on the current soil profile, remaining soft soil thickness, and pore pressure conditions. These provide valuable inputs for model validation. Figure 12 compares the model-predicted deformed mesh and excess pore pressure distribution in 2023 with the CPTu profiles and dissipation test results. The close agreement demonstrates that the model reliably replicates site behaviour, confirming its suitability for evaluating the impact of the zone of 'missing' PVDs beneath Bund 4, forecasting post-construction settlement under current and future loading scenarios.

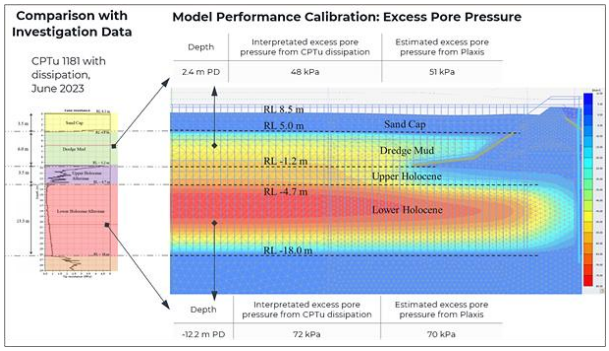

Figure 12. Comparison of FEM predictions and CPTu in 2023

Preliminary 1D analyses indicated that PCS criteria might not be achieved. However, the calibrated 2D FEM model predicts that settlement remains within acceptable limits without the need for further ground treatment, as shown in Figure 13. This improved performance is attributed to the 2D FEM model ability to capture complex interactions, including historical construction sequences, the preload effect of the bund, and radial drainage toward PVDs installed in adjacent paddocks. These factors accelerate consolidation in the LHC, placing it in a slightly over-consolidated state following surcharge removal, thereby reducing long-term settlement.

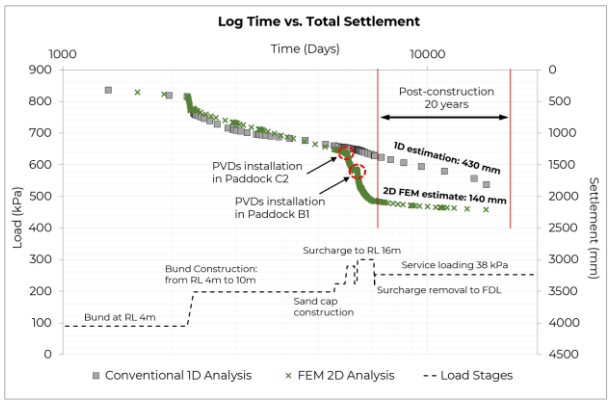

Figure 13. Comparison of conventional 1D and 2D FEM outcome

6 ENGINEERING OUTCOMES AND BROADER IMPLICATIONS

This study resulted in PoB reducing the installation footprint of PVDs and associated pre-drilling requirements. The zone that was impacted by the bund was approximately 10 m wide and 200 m in length. Considering the triangular grid and spacing of 1.25 m between each PVD location, this resulted in the potential for pre-drilling and PVD installation of 1,478 locations for approximately 42,000 lineal metres of PVDs. Pre-drilling through the bund material would have resulted in the mobilisation of a 'heavy' pre-drilling rig to reach the target depths. Mobilisation of such a rig would have been a significant project cost, along with the delays to the project schedule. The production of the pre-drilling works would only allow 70 to 90 locations per shift, compared to between 300 to 500 PVDs per shift, thus slowing down the production of PVD installation. This would result in delays of up to 18 days of installation time, and time required to mobilise the pre-drilling rig.

For future ground improvement campaigns at reclamation areas on soft soils, the installation of PVDs may not be required or at a reduced extent, where bund walls have been constructed for long periods of time prior to surcharging, as they can act as a 'pre-load' to the underlying compressible soils. This will reduce the requirement for PVDs being installed (less material use for a more sustainable design), and also reduce the risk of installing PVDs through hard or dense materials that aren't suitable for PVD installation. Numerical analysis and calibration using observational approaches are recommended to provide confidence in these more complex situations where 1D consolidation analysis and assumptions require refinement.

7 CONCLUSIONS

This study demonstrates how integrating advanced numerical modelling with a field-calibrated approach can guide decision-making for complex ground improvement projects. By applying a fully staged FEM approach with an advanced constitutive model, the research representatively captured the complex drainage, consolidation, and creep interactions at the PoB. Replicating observed settlement, pore pressure dissipation, and strength gain provided technical assurance and the confidence to move beyond conventional design assumptions when justified by site-specific evidence. More broadly, the findings highlight advanced geotechnical modelling as a key tool for both risk management and value optimisation. For large-scale reclamation works on challenging ground, particularly where long-standing preload structures and variable drainage conditions exist, such modelling enables performance-driven solutions that improve constructability and reduce material use. This approach reflects contemporary practice, where robust numerical analysis, supported by targeted field validation, underpins safe, economical, and sustainable outcomes.

8 ACKNOWLEDGEMENTS

The authors wish to thank Dr Jay Ameratunga for his review and constructive feedback on the paper.

9 REFERENCES

Alinur, J., Perryman, G., Ng, Z. and Chan, C., 2023. Geotechnical design and monitoring of FPE seawall upgrade (second top-up), Port of Brisbane. *Proc. 14th ANZGEO*, Cairns.

Barron, R.A., 1948. Consolidation of fine-grained soils by drain wells. *Transactions of the American Society of Civil Engineers*.

Brinkgreve, R.B.J., Kumarswamy, S., Swolfs, W.M., et al., 2023. *PLAXIS 2D Reference Manual*.

CUR 191, 1997. Design of vertical drains. The Netherlands: CUR.

Indraratna, B., Rujikiatkamjorn, C. and Sathananthan, I., 2005. Analytical and numerical solutions for a single vertical drain including the effects of vacuum preloading. *Canadian Geotechnical Journal*, 42(4), pp.994–1014.

Mesri, G., 1994. Secondary compression and creep in soils: 50th Rankine Lecture. *Géotechnique*, 44(2), pp.215–247.

Mesri, G. and Castro, A., 1987. Cα concept and K₀ during secondary compression. *Journal of Geotechnical Engineering*.

Ng, Z., Dissanayake, K., Ameratunga, J. and Honeyfield, N., 2016. Port of Brisbane clay characteristics and correlations with back analysis results. *Proc. 19th Southeast Asian Geotechnical Conference & 2nd AGSEA Conference*, Kuala Lumpur.

Tibbets, I.R., Hall, N.J. and Dennison, W.C., 1998. Moreton Bay and catchment. *School of Marine Science*, University of Queensland.

Vermeer, P.A. and Neher, H.P., 1999. A soft soil model that accounts for creep. *Beyond 2000 in Computational Geotechnics*, Amsterdam: Balkema, pp.249–261.